atmosphere

MDPI

Article

An Integrated Estimating Approach for Design Wind Speed under Extreme Wind Climate in the Yangtze River Inland Waterway

Juanjuan Li [1,2], Lijun Liu [1,2,*], Youjia Liang [3], Chao He [1,2] and Jiming Jin [1,2]

[1] College of Resources and Environment, Yangtze University, Wuhan 430100, China
[2] Hubei Key Laboratory of Petroleum Geochemistry and Environment, Yangtze University, Wuhan 430100, China
[3] School of Resources and Environmental Engineering, Wuhan University of Technology, Wuhan 430070, China
* Correspondence: liulijun@yangtzeu.edu.cn; Tel.: +86-136-1939-3410

Abstract: Developing the engineering design standard of wind speed is a key aspect of the climate research in the Yangtze River Inland Waterway (YRIW), which is highly sensitive to extreme weather and climate processes. An engineering design wind speed projection model was established to evaluate the distribution of extreme wind speeds in the YRIW region at spatiotemporal scales from 1979 to 2100, integrating the Weibull distribution and generalized extreme value (GEV) distribution characteristics. We also used high-precision climate model products and integrated analysis methods to predict the evolution of engineering design wind speeds in the study area in the future. The results show that: (1) The maximum wind speed in the study area shows a decline—recovery trend in the historical period in general and a weak increase in Wuhan and Shanghai. (2) The maximum wind speed does not follow the Weibull distribution, and the extracted extreme wind speed types include type I, II, and III GEV distributions. (3) The updated inland port project design wind speed can meet the climatic and topographic characteristics of the YRIW. (4) The model of CNRM-CM6-1-HR product accurately captures the spatial and temporal characteristics of the maximum wind speed. (5) In the future, the design wind speed shows a slight decrease in Shanghai, Jiujiang and Yueyang. These findings provide a scientific theoretical reference and engineering reference for the development of design wind speeds for inland port projects at various cross-sections in the YRIW.

Keywords: climate change; design wind speed; wind extremes; inland port; Weibull; GEV

Citation: Li, J.; Liu, L.; Liang, Y.; He, C.; Jin, J. An Integrated Estimating Approach for Design Wind Speed under Extreme Wind Climate in the Yangtze River Inland Waterway. *Atmosphere* **2022**, *13*, 1849. https://doi.org/10.3390/atmos13111849

Academic Editors: Yun-Cheng He, Ying-Hou He and Yong Cao

Received: 10 October 2022
Accepted: 4 November 2022
Published: 7 November 2022

1. Introduction

The Yangtze River Inland Waterway (YRIW) in China is an important transportation hub for global shipping trade and economic development [1]. Due to climate change, frequent extreme wind events and their secondary disasters (e.g., power disruptions, bridge damage, ship accidents) have become major disruptive weather and climate events in Yangtze River inland, especially for some large ports [2]. In recent years, stakeholders such as climate scientists and government administrations have begun to pay sustained attention to the impact of extreme wind events in relation to port engineering design [3]. Extreme wind events of different frequencies and intensities (e.g., strong winds and storms) cause far more damage to inland river ports than other disasters, severely affecting the infrastructure safety of inland ports [4,5] and having a significant negative impact on the socioeconomic development of the Yangtze River Economic Zone [6]. Therefore, it is important to study the design wind speed of port projects for the development of inland river navigation specifications and navigational safety management of the Yangtze River.

The estimation of extreme wind speeds for different recurrence periods can accurately obtain wind loads and provide a reference for the safety specification of wind structure design in port engineering [7,8]. The calculation method of extreme wind speed is mainly

to fit the port wind speed data into a probability distribution function [9], including steps of wind speed sample extraction, probability distribution modelling and parameter estimation and testing [10]. Wind speed sample extraction mainly includes methods such as Tukey, Beard and Foster, Adamowski, Gringorten, Hazen, Laplace and Filliben [11]. A common probability distribution model suitable for estimating a wide range of wind speeds is the Weibull distribution [12], which provides a good fit to the rightmost tail distribution of wind speeds but suffers from the problem of misestimation of the tail distribution of wind speeds when estimating the extreme value distribution in a data set [13]. The generalised extreme value (GEV) model is the main method used specifically to estimate extreme wind speed distributions at different spatial and temporal scales, with three main distribution forms, of which the Gumbel distribution (type I) is again the most commonly used for fitting extreme wind speed distributions [14]. The advantage of this method is that it is easy to implement, but the sample utilization rate is low, and it is mainly suitable for areas with long-term wind speed observations, and should also be used in combination with other methods in cases of short time series and strong wind-climate mixing. The method is recommended by the Canadian Code for Structural Loads in Buildings (CNBC 1995) and the GB50009-2012 code in China [15]. Parameter estimation and testing methods for the GEV distribution function include minimum mean square error (MMSE), maximum likelihood (ML), method of moments (MOM), probability weighted moments (PWM), linear moments (LM) and least squares (LS) [16]. In contrast to the generalisability of the Weibull method, the GEV distribution is only applicable to the estimation of extreme values (especially annual maxima). Therefore, there is still a need to explore the development of a comprehensive estimation method for extreme wind speeds applicable to the complex geoclimatic environment of the Yangtze River, which can provide engineering parameters and methodological support for the development of wind speed standards for inland river port projects on the Yangtze River.

Extreme wind speed studies are showing a trend in modelling. Model scenario simulations all show decreasing surface wind speeds globally and in specific regions ("global quiescence"); for example, the mean surface wind speed in the Northern Indian Ocean will decrease significantly in the mid- to late 21st century under RCP4.5 and 8.5 conditions [17]. However, CMIP5 was used to reveal the annual maximum wind speed and its return period in the North Sea, and the frequency of extreme wind events continued to increase globally [18,19]. Therefore, it is particularly important to study how the navigable environment of the YRIW adapts to global climate change. The reliability of the model data must therefore be high and effective in describing the spatial and temporal dynamics of the atmosphere, wind and waves that affect the navigable environment. To the best of our knowledge, the emerging High Resolution Model Intercomparison Project (HighResMIP) with a more sophisticated mechanism has been able to provide assessment support for GCMs at 25–50 km horizontal resolution; 14 model data sets from HighResMIP have been validated and effectively applied on a regional scale, and model evaluation found that CNRM-CM6-1-HR simulates wind speeds better than other models [20].

In this study, we obtained long-time-series weather station data (1979–2020) and CNRM-CM6-1-HR climate model data, including historical (1979–2014) and future period (2015–2100). Then, an integrated modelling approach was developed for design wind speed estimation by integrating the Tukey method and the Weibull-GEV distribution. Specifically, we aimed to (1) reveal the spatial distribution characteristics of engineering design wind speeds in inland ports at the annual-seasonal scales during historical periods; (2) evaluate the reliability of the updated engineering design wind speeds compared with the existing normative standard; (3) assess the availability of CNRM-CM6-1-HR in the study area using an accuracy validation method based on observations and high-precision model data; and (4) calculate the 10/50/100-year return periods of engineering design wind speeds in the nine inland ports of the YRIW from 1979 to 2100, and climate adaptation countermeasures based on extreme weather events are also discussed.

2. Information and Methods

2.1. Data

Nine representative ports along the Yangtze River inland waterway (YRIW) (104°28′1″–121°54′10″ E and 27°39′30″–32°42′28″ N) were selected (Figure 1), including: Shanghai Port, Nanjing Port, Anqing Port, Jiujiang Port, Wuhan Port, Yueyang Port, Yichang Port, Chongqing Port and Yibin Port, which are affected by the complex and variable geographical and climatic environments along the YRIW [21]. The meteorological station observations were obtained from the Global Surface Summary of the Day (GSOD) data set (1979–2020, http://www.climate.gov/ (accessed on 9 October 2022)), which undergoes automated data quality control with multiple processes to better eliminate data random errors and mistakes [22]. Information from meteorological stations at nine ports was obtained, and the data selection criteria were to satisfy both temporal continuity and data integrity for wind speed analysis. The daily maximum wind speed V_{max} at each station was extracted using Matlab 2019a programming, and the data set used for wind speed analysis was formed by preprocessing.

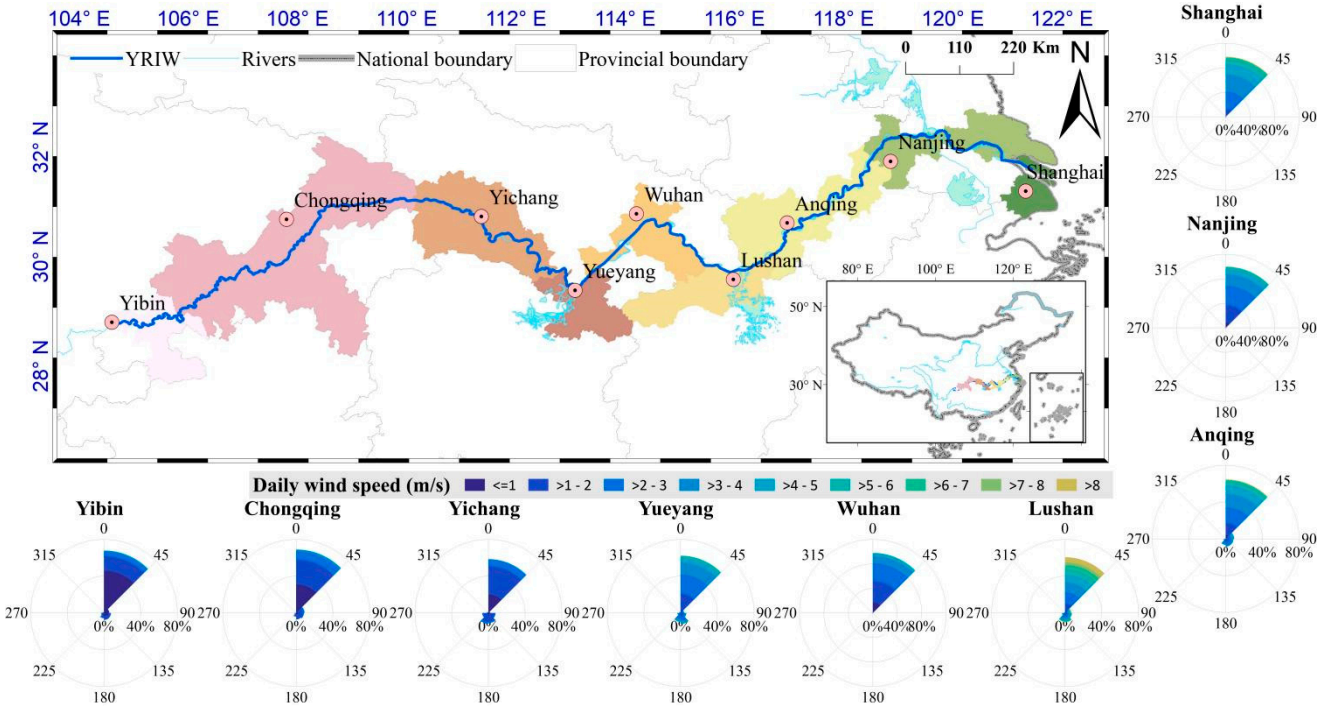

Figure 1. Location and wind–rose of the weather observing stations in the Yangtze River inland ports.

Daily maximum wind speeds are obtained from the CNRM-CM6-1-HR climate model for the historical scenario (1979–2014) and the Highres-future scenario (2015–2100) with a spatial and temporal resolution of daily and ~50 km. The model is the highest-resolution version of the CNRM-CM6.1 model jointly produced by the French National Centre for Meteorological Research (CNRM) and the European Research Centre of the French Centre for Computational Sciences (CERFACS) and is an important component of the HighResMIP and DECK experiments in CMIP6 (http://www.umr--cnrm.fr/cmip6/ (accessed on 9 October 2022)). 14 sets of model data from HighResMIP have been applied to Atlantic tropical cyclone studies, but Chinese regional applications are still lacking, and model evaluation found that CNRM-CM6–1-HR simulates wind speeds better than other models.

2.2. Weibull–Tukey Sampling Method

A two-parameter Weibull distribution is used to obtain the wind speed characteristics of the port (Equations (1)–(4)). The wind speed distribution is obtained through the cumulative distribution function $y_W(x)$ and the probability density function $y_W(x)'$ of the random variable x [23]. The model fit is tested using a quantile Q–Q plot of the Weibull distribution values and the actual wind speed, and then different wind speed probability distributions are determined according to the wind speed threshold: wind speeds below a specific threshold follow the Weibull distribution, otherwise the GEV distribution [24]. The threshold discrimination method is the Tukey method (Equations (5) and (6)) [25].

$$y_W(x) = 1 - exp\left[-\left(\frac{x}{\Sigma_W}\right)^{k_W}\right] \tag{1}$$

$$y_W(x)' = \frac{k_W}{\Sigma_W}\left(\frac{x}{\Sigma_W}\right)^{k_W-1} exp\left(-\left(\frac{x}{\Sigma_W}\right)^{k_W}\right) \tag{2}$$

$$\Sigma_W = \frac{m}{\Gamma(1+1/k_W)} \tag{3}$$

$$k_W = \left[\frac{m}{\sigma}\right]^{1.086} \tag{4}$$

$$h_{0.25} = k_W[ln(4) - ln(3)]^{1/\sigma_W} \tag{5}$$

$$h_{0.75} = k_W[ln(4)]^{1/\sigma_W} \tag{6}$$

where Σ_W and k_W denote the scale and shape parameters of the wind speed, respectively. m is the mean, σ is the standard deviation, Γ is the gamma function and $h_{0.25}$ and $h_{0.75}$ are the lower- and higher-order quartiles of the Weibull distribution using h to denote the quartile interval of the wind speed ($h = h_{0.75} - h_{0.25}$), considering that wind speed greater than $h_{0.75} + 1.5h$ is considered extreme. The obtained extreme wind speed is used for GEV distribution calculation.

2.3. Design Wind Speed Estimation

First, using the extreme wind speed sampling data x' of the cumulative distribution function $y_G(x)$ to represent the GEV distribution,

$$y_G(x') = \begin{cases} exp[-exp(-y)] & k = 0 \\ exp\left[-(1-ky)^{\frac{1}{k}}\right] & k \neq 0 \end{cases} \tag{7}$$

$$\Sigma' = \left[(2b_1 - m')k'\right] \Big/ \left[\Gamma\left(1 - c^{-k'}\right)(1+k')\right] \tag{8}$$

$$\mu' = m' + \left\{\Sigma\left[\Gamma(1+k') - 1\right]\right\}/k' \tag{9}$$

$$k' = 7.895c + 2.9554c^2 \tag{10}$$

$$c = \left[(2b_1 - m')/(3b_2 - m')\right] - [ln2/ln3] \tag{11}$$

where y is the normalized variable. When the shape parameter k = 0 for the Gumbel distribution, $y = (x' - \mu_G)/\Sigma_G$ using the MOM estimator to obtain the scale parameter ($\Sigma_G = \sigma'\sqrt{6}/\pi$) and the location parameter ($\mu_G = m' - 0.5772\Sigma_G$), which uses the mean of the sample m' and standard deviation σ' for parameter estimation, which is computationally convenient and reliable [26]. When $k < 0$, the Fréchet distribution is used, and otherwise it is the inverse Weibull distribution, both using the PWM estimator to calculate the parameters Σ', μ' and k' [27]. $y = (x' - \mu')/\Sigma'$, b_1 and b_2 are denoted respectively as $\sum_{j=1}^{n-1}\left[(n-1)x'_j/n(n-1)\right]$ and $\sum_{j=1}^{n-1}\left[(n-j)(n-j-1)x'_j/n(n-1)(n-2)\right]$, and n is the sample size.

Then, the goodness of fit of the model was tested using R^2 and *RMSE*. When R^2 is 0–1, the closer the value is to 1, the more reasonable the distribution model describing the data is; the closer *RMSE* is to 0, the better the model is:

$$R^2 = 1 - \left(\frac{\sum_{i=1}^{n} \left(y'_{i,o} - y'_{i,t} \right)^2}{\sum_{i=1}^{n} \left(y'_{i,o} - \overline{y'_{i,t}} \right)^2} \right) \tag{12}$$

$$RMSE = \frac{\sqrt{\sum_{i=1}^{n} \left(y'_{i,o} - y'_{i,t} \right)^2}}{n - \tau} \tag{13}$$

$$y'_{i,o} = \begin{cases} -ln(-ln(y_G(x))) & k = 0 \\ (-In(y_G(x)))^{k'} & k \neq 0 \end{cases} \tag{14}$$

$$y'_{i,t} = \begin{cases} 0.5772 + \frac{\pi}{\sqrt{6}} \frac{x - m'}{\sigma'} & k = 0 \\ \Sigma' - \mu' \left(\frac{x - m'}{\sigma'} \right) & k \neq 0 \end{cases} \tag{15}$$

where $y'_{i,o}$ and $y'_{i,t}$ are the theoretical cumulative distribution function values of GEV for extreme wind speeds, respectively, the number of fitted parameters in the Gumbel distribution $\tau = 2$, and in the Fréchet and inverse Weibull distributions $\tau = 3$. The curves of $y'_{i,t}$ are stepped, jumping up by a factor of 1/n when the extreme wind speed values at each port are repeated. $y_G(x)$, Σ' and μ' from Equations (7)–(9).

Finally, the error-minimizing GEV distribution model is used to derive T-year (10/50/100) recurrence periods for the annual scale, dry (December–February), normal (March–May and October–November), and flood (June–September) periods for a given port Engineering design wind speed (V_d).

$$V_d = \mu - \Sigma \cdot ln[-ln(1 - 1/T)] \tag{16}$$

The CNRM-CM6-1-HR model data of the navigable environment of the YRIW were extracted, and the daily maximum wind speed data of the historical scenario and the Highres-future scenario were processed on an annual or seasonal scale, respectively; then, the extreme wind speeds of the YRIW above a specific threshold were fitted by applying the type I, II and III GEV distributions. Then extrapolate V_{dhis} and V_{dfut} for the 10/50/100-year return periods of the historical and Highres-future scenarios, and finally compare and analyse the temporal and spatial heterogeneity changes in extreme wind speeds for different return periods:

$$cv = V_{dfut} / V_{dhis} \tag{17}$$

where *cv* is the coefficients of variation between V_{dhis} and V_{dfut}, which is used to determine the relative variability of different extreme wind speed data sets under climate change for the nine sections of the YRIW.

3. Results

3.1. Spatial Characterization of Maximum Wind Speeds

The trends in spatial distribution in the maximum wind speeds were extracted on the annual and seasonal scales by calculating the multiyear average changes in wind speeds at the major stations in the upper, middle and lower Yangzi River from 1979 to 2020 (Figure 2). In terms of spatial distribution, the regional annual distribution of maximum wind speed reflects the spatial characteristics of large nearshore and small inland, such as a large area of high maximum wind speed (>9 $m \cdot s^{-1}$) in the downstream (Anqing–Shanghai) section and a low maximum wind speed zone (<7 $m \cdot s^{-1}$) in the upstream Yibin–Yichang section, except for the Yibin section, where the wind speed reaches its maximum (11 $m \cdot s^{-1}$). The Yueyang–Wuhan section and the Jiujiang section are sub–maximum wind centres, where

the Yueyang–Wuhan section reaches its maximum (8–9 m·s^{-1}) during the flood season, and the Jiujiang section reaches its maximum (5–13 m·s^{-1}) during the dry season.

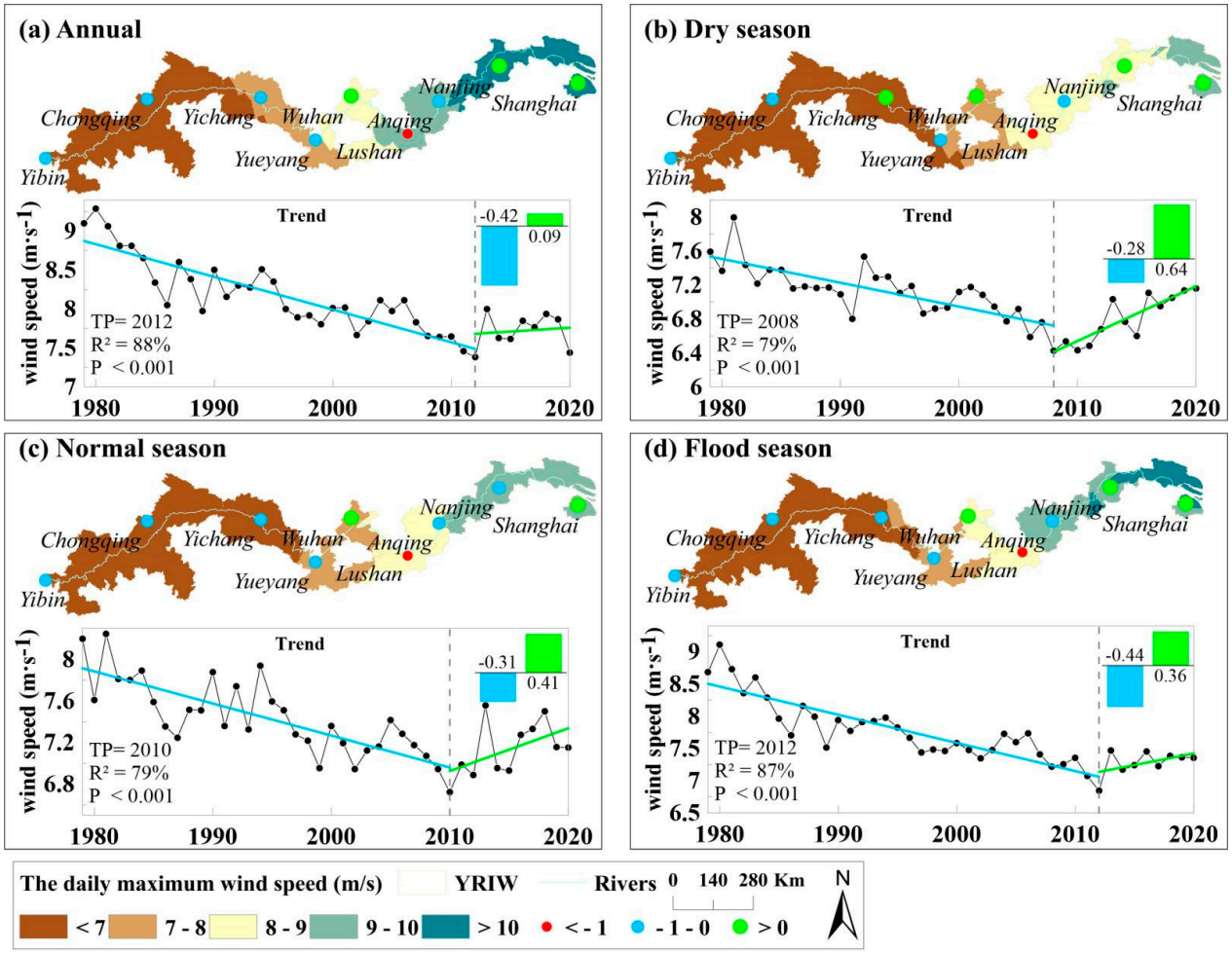

Figure 2. Spatial distribution and trend of daily maximum wind speed at nine ports along the YRIW from 1979–2020.

Analyzing the annual trend rate changes in the maximum wind speed along the line, the overall values are negative except for positive values at Wuhan, Nanjing and Shanghai stations, indicating a weak upward trend (>0) and a weak downward trend (>–2.0 m·s^{-1}·decade^{-1} at all stations in the offshore section; except for a positive trend at Yichang, Wuhan, Nanjing and Shanghai (>0) in the dry season, all other areas have a negative trend, including about –1.0 m·s^{-1}·decade^{-1} at Anqing, with little change at the remaining stations. This indicates that the maximum wind speed at Anqing has a weak decreasing trend in the dry season; except for the dry season, the distribution pattern of the tendency in other seasons is similar to that of the whole year, especially the positive tendency in Wuhan (0.8 m·s^{-1}·decade^{-1}), Nanjing (0.4 m·s^{-1}·decade^{-1}) and Shanghai (1.0 m·s^{-1}·decade^{-1}) stations during the flood season, and the negative tendency in the rest of the stations. In general, the maximum wind speed in the YRIW shows a decline (−0.42 m·s^{-1}·decade^{-1})–recovery (0.09 m·s^{-1}·decade^{-1}) trend in the historical period, with Wuhan, Nanjing and Shanghai stations showing a slight increase except for the dry season.

3.2. Extreme Wind Speed Variations Based on the Weibull Distribution

The daily maximum wind speed (Vmax) Weibull probability density distribution was further calculated and fitted for each port to obtain the wind speed curve (Figure 3), and the accuracy of the Weibull distribution function was examined using a quantified Q–Q plot (Figure 4). It was found that the high-frequency wind speed variation was mainly below 20 m·s^{-1}; the raw frequency values of Vmax were much higher than the fitted values for all ports except Nanjing, Anqing, Jiujiang and Wuhan; and it was also found that the deviation between the two was larger in the wind speed interval below 10 m·s^{-1}, indicating that the Weibull distribution results of these ports were susceptible to the influence of extreme wind speeds. The maximum wind speeds at Jiujiang port were closest to the Weibull distribution, and the other ports showed large deviations between the data set and the 45° line after exceeding a certain maximum wind speed. For example, the wind speed data of Shanghai port, Nanjing port and Anqing port in the interval above 20 m·s^{-1} do not obey the Weibull distribution, the wind speed data of Wuhan port and Yueyang port in the interval above 17 m·s^{-1} do not obey the Weibull distribution, and the wind speed data of Yichang port, Chongqing port and Yibin port in the interval above 10 m·s^{-1} do not obey the Weibull distribution. In general, there are extreme wind speeds in the maximum wind speed distribution of each port, which affects the smoothness characteristics of the Weibull distribution. Therefore, the sample data sets of extreme wind speeds for each port were extracted from the wind speed data that do not conform to the Weibull distribution and used to fit the GEV distribution, with the highest sample thresholds for Jiujiang port (10.15 m·s^{-1}) and Shanghai port (7.25 m·s^{-1}) and the lowest for Yibin port (2.82 m·s^{-1}).

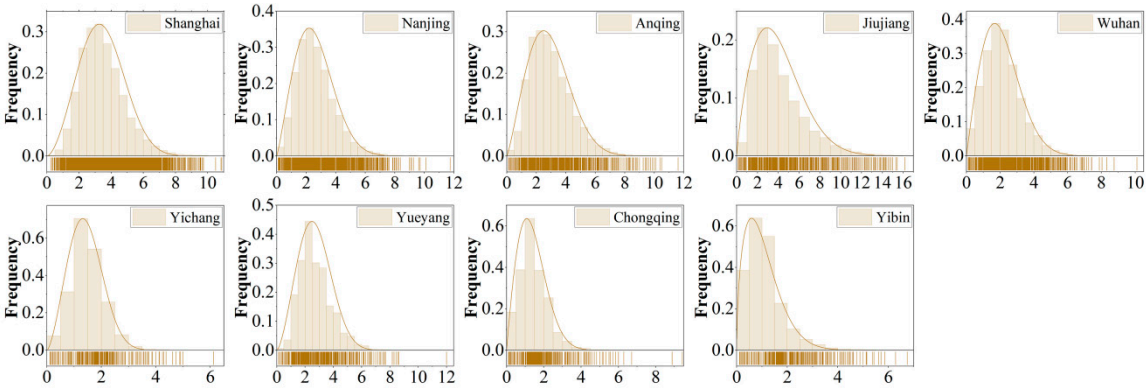

Figure 3. The frequency statistical histogram and the Weibull distribution of maximum wind speed (Unit: m·s^{-1}) for nine ports, 1979–2020.

3.3. Design Wind Speed Analysis Based on GEV Distribution

The probability plots of the cumulative GEV distribution of extreme wind speeds at each port along the YRIW from 1979 to 2020 show that the fitted theoretical wind speeds exhibit a high degree of agreement with the observed wind speeds (Figure 5). The high-frequency wind speed variations are mainly concentrated in the wind speed interval within 20 m·s^{-1}, and the daily maximum wind speeds of each port in the fitted results follow the GEV distribution; except for the wind speed of Jiujiang port, which is concentrated in the range of 10–20 m·s^{-1}, the theoretical cumulative distribution function curves of the ports show a flattening feature in the interval where the cumulative probability is above 0.9. The probability of extreme wind speed distribution around 10 m·s^{-1} is higher in Shanghai, Nanjing and Anqing ports, 7 m·s^{-1} in Wuhan and Yueyang ports, 5 m·s^{-1} in Yichang and Chongqing ports, and 3 m·s^{-1} in Yibin port.

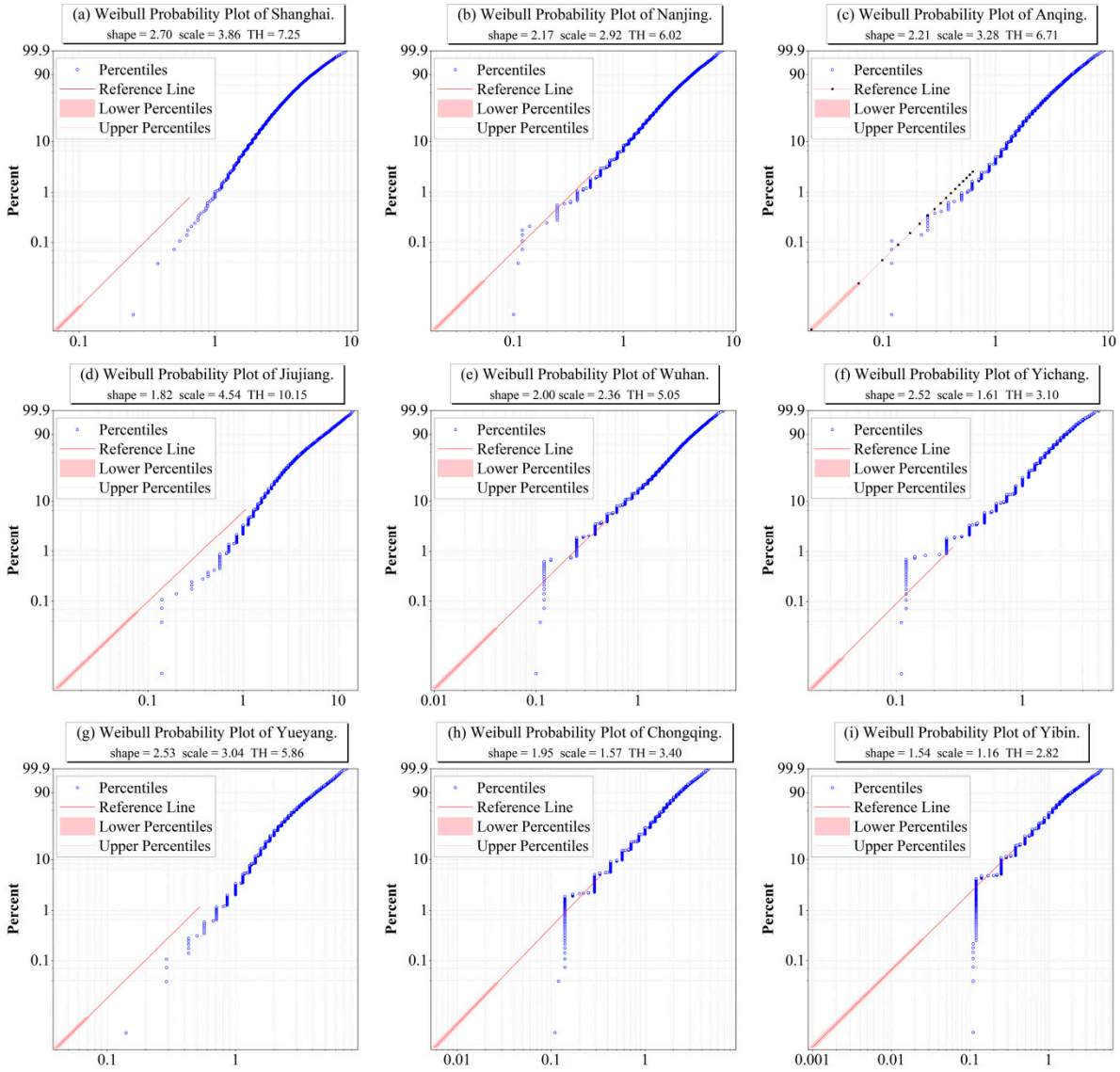

Figure 4. Q–Q plots of the Weibull distribution for nine ports, 1979–2020.

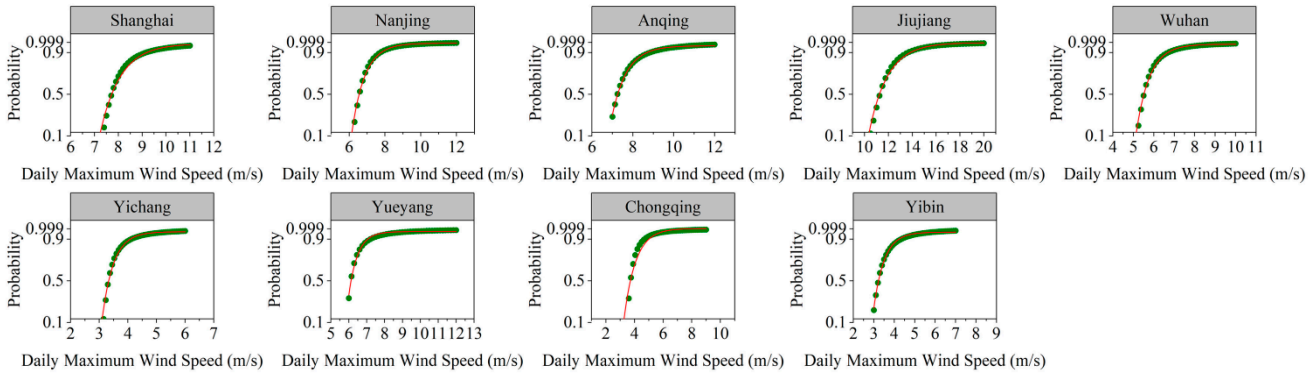

Figure 5. Probability–wind speed plots of the cumulative GEV distribution for nine ports from 1979–2020 (Dotted line: observed wind speed; red line: theoretical wind speed).

The extreme wind speeds during the dry (December–February), normal (March–May & October–November), flood (June–September) and annual periods of the Yangtze River inland waterway from 1979–2020 were extracted to test the goodness of fit of the GEV distribution type, and the fitted V_d estimates for different seasons in the study area were derived

according to the above method (Figure 6b). R^2 (both greater than 0.9) and *RMSE* indicated that the annual- and seasonal-scale theoretical distributions were in good agreement with the measured data, which indicated that the estimated V_d was highly reliable. Among them, R^2 for Wuhan, Yichang and Chongqing are all higher than 0.96, indicating a good fit to the GEV distribution; the R^2 values for the remaining ports are all higher than 0.8, with good fitting performance and *RMSE* less than 1; only the *RMSE* of Jiujiang is 1.78 m·s^{-1}, which is consistent with the previous results that the wind speed variation and Weibull fitting in the Jiujiang area are better than the theoretical GEV distribution.

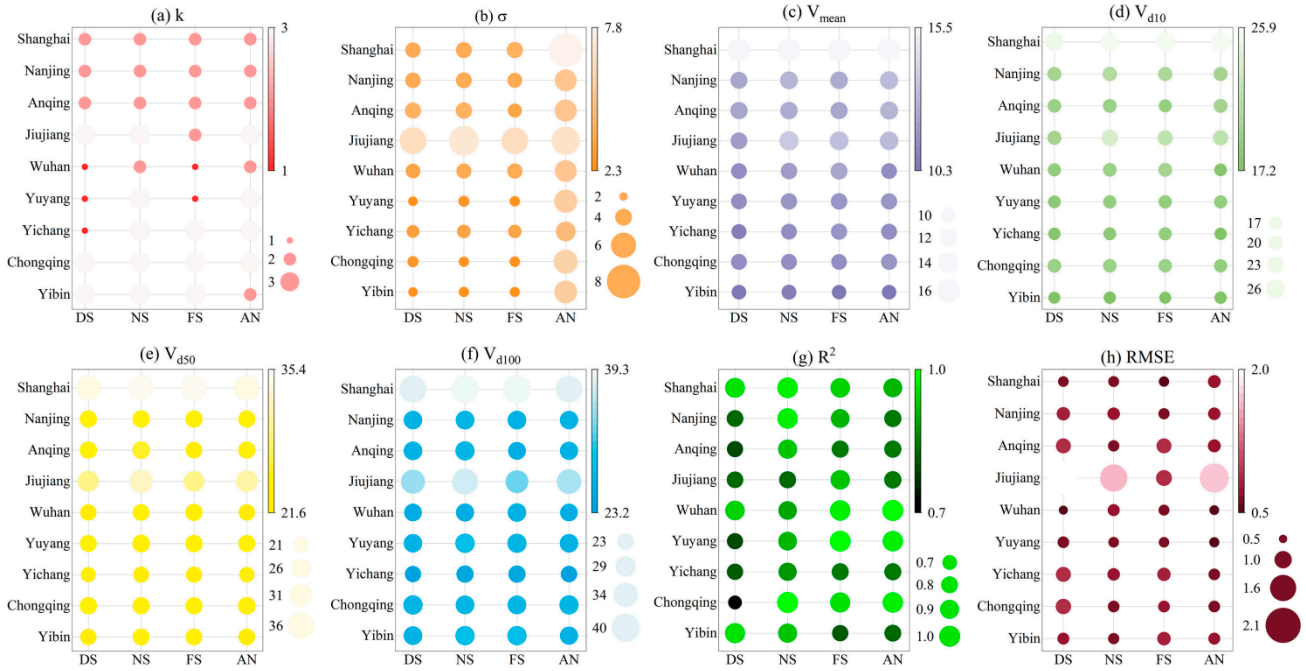

Figure 6. (**a**–**h**) Goodness-of-fit tests for the GEV distribution and 10/50/100 engineering design wind speeds (DS = dry season, NS = normal season, FS = flood season and AN = annual) for nine ports from 1979 to 2020.

1. Annual scale engineering design wind speed

It was found that all ports conformed to the Fréchet distribution (Type II) except for Jiujiang, Yueyang, Yichang and Chongqing, where the distribution type conformed to the inverse Weibull distribution (Type III), indicating that the Gumbel distribution was not applicable to the extrapolation of the annual-scale distribution of extreme wind speeds along the Yangtze River inland waterway, while Types II and III were more applicable to the Yangtze River inland waterway, a region with long time series and strong wind–climate mixing complexity. The mean and variance of the extreme wind speed V_{max} in the YRIW are the largest in Shanghai, 15.53 m·s^{-1} and 7.79 m·s^{-1}, respectively; the smallest in Yibin, 10.32 m·s^{-1}, and the smallest in Yueyang, 4.7 m·s^{-1}. This is consistent with the results of the multiscale analysis in the previous sections, indicating that the wind speed in the YRIW is larger in the middle and down streams. This is consistent with the results of the multiscale analysis in the previous sections that the wind speed along the YRIW is greater in the middle and down streams than in the upper reaches. The wind speed $V_{d10}/V_{d10}/V_{d10}$ of Shanghai port is the highest in the 10/50/100-year return period, and its 100-year scale has the maximum value of 37.5 m·s^{-1} among the three return periods, which may be due to the influence of tropical monsoon climate in coastal area downstream; the next highest area is the maximum value of Jiujiang in the 100-year return period, V_{d100} is estimated to be 35.17 m·s^{-1}, which may be related to the fact that Jiujiang is backed by Mount Lu and adjacent to Poyang Lake, making it subject to the combined influence of lake, land winds and valley winds; the rest of the ports are inland ports, with the lowest 10-year

return periods being Yichang and Yibin, 17.57 m·s^{-1} and 17.5 m·s^{-1}, respectively, with no significant difference; the lowest wind speeds for the 50- and 100-year return periods are Yichang, 21.82 m·s^{-1} and 23.27 m·s^{-1}, respectively.

2. Seasonal-scale engineering design wind speed

The seasonal distributions of upstream Chongqing and Yibin are consistent with the inverse Weibull distribution (type III) in all periods and the Fréchet distribution (type II) in Shanghai, Nanjing and Anqing in all periods downstream, with obvious differences in wind speed distribution between upstream and downstream. For example, the wind speed of Jiujiang in the flood season conforms to the Fréchet distribution, but the dry–normal season conforms to the inverse Weibull distribution; the dry–flood seasons of Wuhan and Yichang both follow Gumbel distribution (Type I), and the normal season conforms to the Fréchet and inverse Weibull distributions; Yueyang only conforms to the Gumbel distribution in the dry season, and the rest are inverse Weibull. The downstream is prone to cyclones by the sea, and the turbulence intensity is much higher than inland, indicating that the Fréchet distribution is applicable to areas with higher storm frequency. In addition, the Fréchet distribution is still present in Wuhan under the influence of tropical cyclones, where frequent catastrophic gales occur in spring due to climate change.

The seasonal scale recurrence period projection shows that V_{d10} (25.61–19.88 m·s^{-1}), V_{d50} (35.31–24.55 m·s^{-1}) and V_{d100} (39.23–26.53 m·s^{-1}) are higher in the Shanghai–Wuhan port during the flood season than in other periods, and the high wind speed in the flood season is related to the strong convective weather caused by the prevailing southeastern summer wind, and the prevailing subtropical high pressure and the accompanying V_{d10} (19.58–17.24 m·s^{-1}), V_{d50} (25.05–23.32 m·s^{-1}) and V_{d100} (27.60–26.70 m·s^{-1}) are higher than other periods during the dry period in Chongqing–Yibin port because the winter temperature in Sichuan–Chongqing area is high and the stronger warm and humid air meets with the cold air from the north to cause windy weather. The V_{d10}, V_{d50} and $V_{d100\,\mathrm{of}}$ the remaining ports are significantly higher than their respective other periods, and the design wind speed $V_{d100\,\mathrm{is}}$ mostly in the range of 25–27 m·s^{-1} except for Jiujiang (36.99 m·s^{-1}), which is due to the higher average temperature in March–April and the high-pressure gradient compared with other seasons, resulting in higher wind speed.

3.4. Assessment of the Effect of Projection of Engineering Design Wind Speed

The above results show that Fréchet distribution can be widely used to simulate extreme wind speeds downstream of the YRIW, while the inverse Weibull distribution is mostly suitable for the upstream, and a mixed distribution of multiple GEV types exists in the midstream. The original data are the design wind pressure tables including major cities in China, from which the wind pressure values of the cities where the ports of different YRIWs are located were extracted (Figure 7) and converted to the design wind speed of the ports according to $P_d = V_d^2/c$ to port project design wind speed: *Pd* is the design wind pressure value (kN/m^2), V_d is the design wind speed (m·s^{-1}), c = 1600. Multiyear extreme wind speeds V_{d10}, V_{d50} and V_{d100} were used to compare with the recurrence period extreme wind speeds ($V_{d10\mathrm{old}}$, $V_{d50\mathrm{old}}$ and $V_{d100\mathrm{old}}$) of the Code.

Among them, the design wind speed of Shanghai specification project is the highest in all ports, with $V_{d10\mathrm{old}}$, $V_{d50\mathrm{old}}$ and $V_{d100\mathrm{old}}$ of 25.3 m·s^{-1}, 29.66 m·s^{-1} and 30.98 m·s^{-1}, respectively, and the Fréchet distribution projected design wind speeds of V_{d10}, V_{d50} and V_{d100} of 25.88 m·s^{-1}, 34.3 m·s^{-1} and 37.5 m·s^{-1}, respectively, with error percentage (E) indicates that the projected design wind speeds are overestimated by 2.28%, 15.63% and 21.04%, respectively, indicating that the Fréchet distribution can detect sensitive wind extremes, reflecting the characteristics of high wind speed growth in Shanghai. The wind speed comparison results vary between coastal and inland storm turbulence intensities along the Yangtze River inland waterway, and the Type I distribution of the Code does not take into account the variability of climate change. The highest V_{d100} in Jiujiang in the middle reaches is 35.17 m·s^{-1}, and the Code design wind speed is 25.3 m·s^{-1}, which is overestimated by 39.02%, probably due to the much greater atmospheric turbulence

transport and higher-intensity turbulence in mountainous areas than in the plains. In addition, the rest of the sites are underestimated. Yibin is in the weak wind region of the mountainous basin with V_{d10old} and $V_{d100old\ of}$ 21.91 m·s^{-1} and 23.66 m·s^{-1}, respectively, and with reverse Weibull distribution winds of 23.65 m·s^{-1} and 26.05 m·s^{-1}, which are overestimated by 7.96% and 10.1%, respectively. The rest of the ports are underestimated, and the reason is related to the overall decrease in the maximum wind speed along the Yangtze River inland waterway. Overall, there are slight differences between the projected V_d and the V_{dold} extracted from the Specification, and the accuracy of data projection can be improved in the future by increasing data samples and improving the spatial and temporal scales to better obtain high precision engineering design wind speeds.

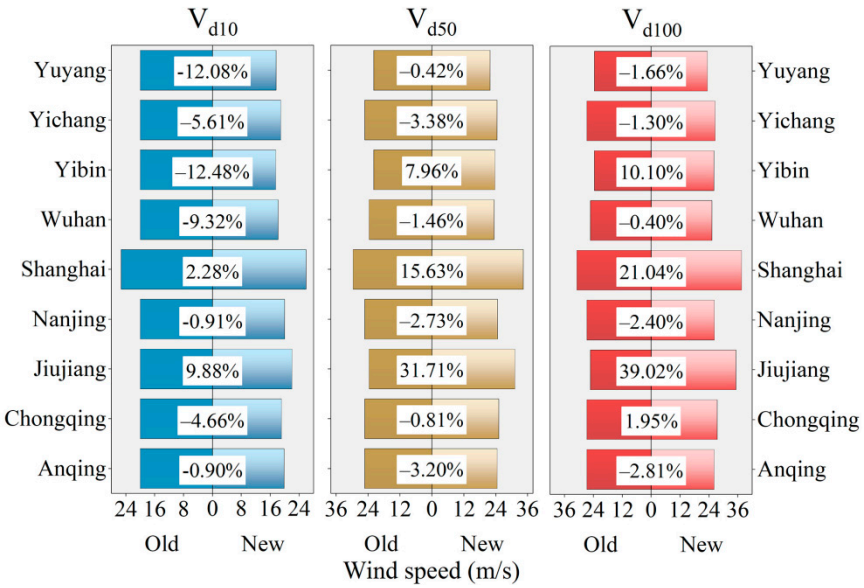

Figure 7. Comparison of 10/50/100 year design wind pressure values, Code design wind speed and updated design wind speed for each area of the YRIW in the Code. Note: old—indicates the design wind speed extracted from the Code; new—indicates the extrapolated design wind speed; E—percentage error.

3.5. Trend Analysis of Extreme Wind Speed Evolution

The maximum wind speed Vmean_sim for the CNRM-CM6–1-HR model for the two average 36–year intervals from 1979–2014 and 2065–2100 was obtained, and its spatial and temporal variation was analysed. The mean and variance of V_{mean_sim} at the annual scale were found to be lower than those at the downscale, but the trend varied among the sections (Figure 8), which was consistent with the distribution of "midstream and downstream being larger than upstream". Further analysis of the seasonal scale shows that the mean and variance of V_{mean_sim} are generally lower in the dry, normal and flood seasons, but still have similar variations to the seasonal scale V_{mean_obs}; this also reflects the characteristic that the mean value of V_{mean_sim} is higher in the dry and normal periods than in the flood season, which is consistent with the seasonal variation of the extreme wind speed data. Overall, the CNRM-CM6–1-HR product captures the temporal variability of regional wind speed more accurately, with the mean and variance of V_{mean_sim} annual scale generally showing a low trend, and the trend varies among the sections, but is in line with the large coastal and small inland distribution.

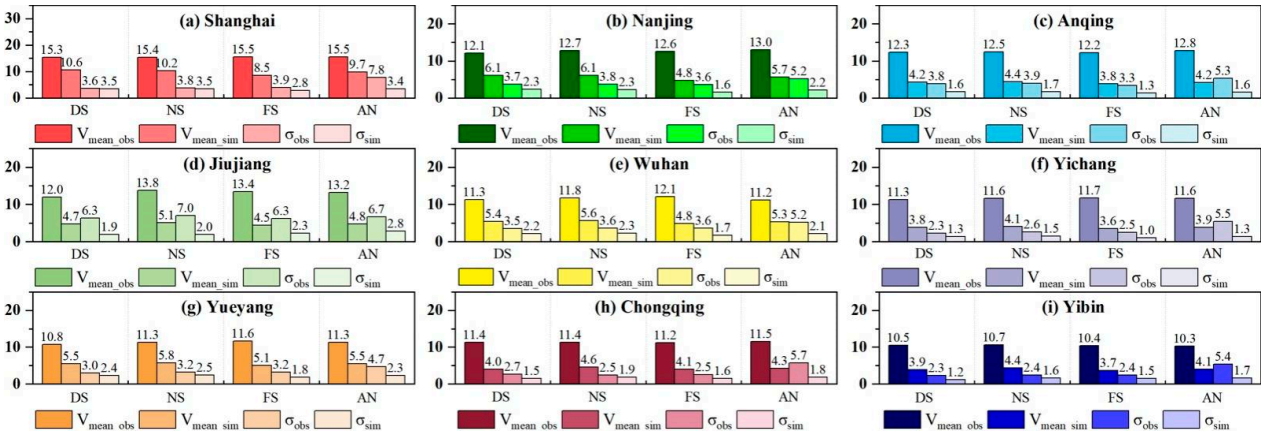

Figure 8. Mean–σ (Unit: m·s^{-1})comparison of seasonal scale (DS = dry season, NS = normal season, FS = flood season and AN = annual) mean of the maximum wind speed from observation and simulation for the two average 36-year intervals from 1979–2014 and 2065–2100 in 9 ports (**a**–**i**).

3.6. Projected Future Changes in Engineering Design Wind Speed

The evolution trend of the extreme wind speed scenario shows that (Figure 9a,e): the future scenario increases compared to the historical scenario V_{mean} wind speed, but the increase is average, for example, the area of the middle and downstream high value centres (Yichang–Yueyang–Wuhan and Nanjing section) increases, while the wind speed in the upstream (Yibin–Chongqing) and Jiujiang decreases instead; the extreme wind speed in the upstream and downstream ports decreases during the dry and normal seasons, while the extreme wind speed in the middle and downstream floods increases, with the highest coefficient of variation in Wuhan (*cv* = 1.033).

The analysis of GEV distribution shape parameters shows that (Figure 9b): (i) the CNRM-CM6-1-HR model is good at capturing the spatial distribution characteristics of extreme wind speeds at the annual scale along the YRIW, but the characterization ability of wind speed distribution characteristics in special climatic regions (e.g., Yibin) still needs to be improved. (ii) The k values of future V_{mean} at the annual scale are –0.083 and –0.057, and the k values of most ports are consistent with the distribution in historical periods; except for Chongqing (*cv* = 0.901), all stations have *cv* > 1, and Yueyang has the largest *cv* of 4.552. (iii) The distribution of extreme wind speeds in the future middle and upper reaches of the navigation section at the seasonal scale is more obviously affected by climate change, with Yibin and Yichang during the flood season k is less than 1 during the flood season, while the rest are greater than 1 in an increasing trend, and the variation is more dramatic during the normal season (Yueyang has the largest k-value variation of –13.046) and the dry season.

The analysis of the location and scale parameters of the GEV distribution shows that the characteristics of the mu high/low value distribution of the future V_{mean} are consistent with the historical period, and all *cv* are greater than 1 (Figure 9b,d). The mu high value centre of the historical period V_{mean} at the seasonal scale is similar to the annual scale distribution, and the spatial distribution of sigma at the annual/seasonal scale is basically similar, with Yichang port as the boundary, with the high value centre to the east and the low value centre to the west, all in line with the "The spatial distribution of sigma at annual/seasonal scales is similar, with the boundary at Yichang port, the high value centre in the east and the low value centre in the west. Nanjing has *cv* less than 1.0 in the annual and normal season, Shanghai has *cv* less than 1.0 in the normal season, and the rest of the sigma values show a large trend.

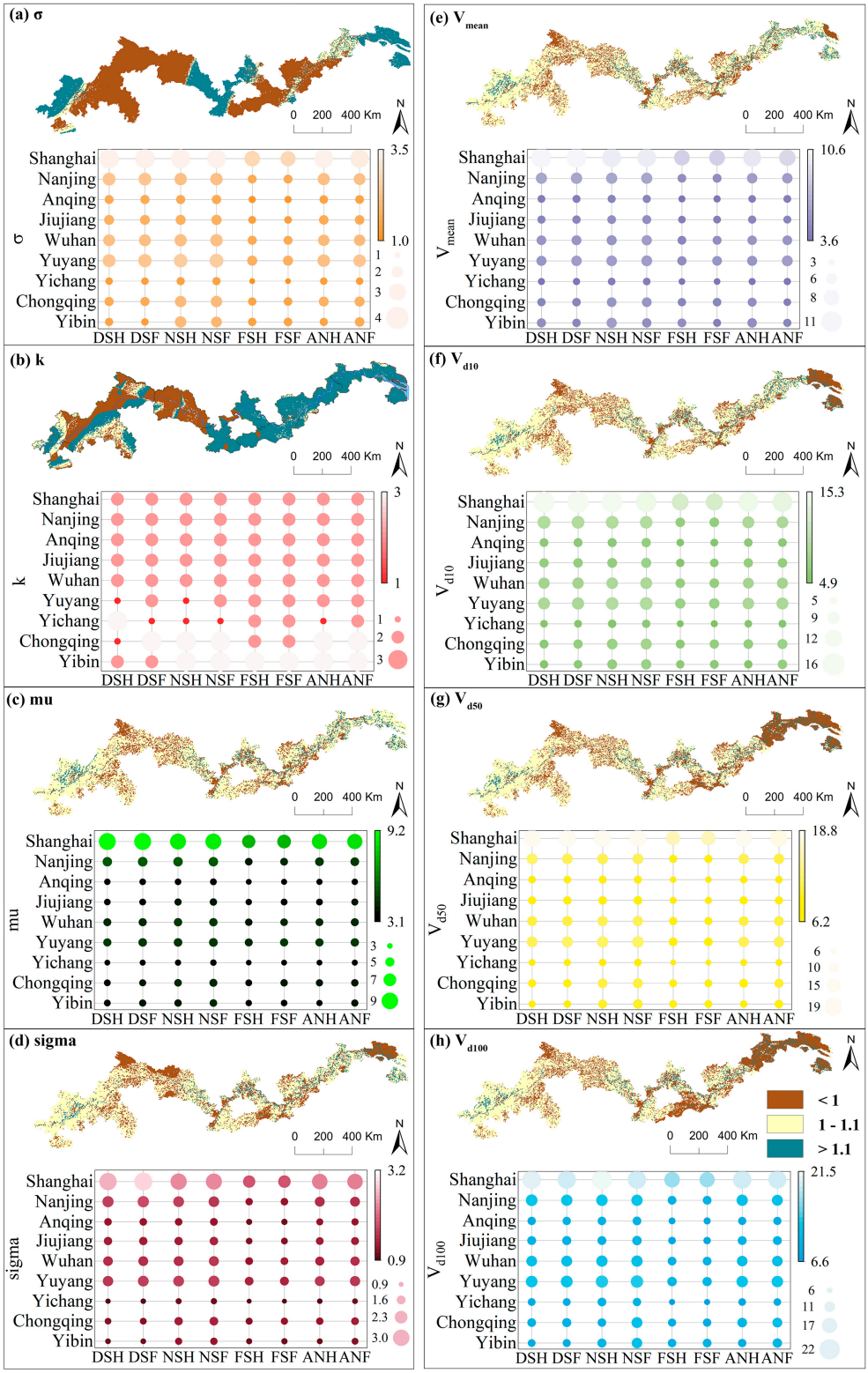

Figure 9. The spatial distribution of the dependent variables σ (**a**), k (**b**), mu (**c**), sigma (**d**), V_{mean} (**e**), V_{d10} (**f**), V_{d50} (**g**) and V_{d100} (**h**) for historical and future periods (annual–seasonal scale); DSH/DSF = dry season in historical/future period, NSH/NSF = normal season in historical/future period, FSH/FSF = flood season in historical/future period and ANH/ANF = annual in historical/future period.

Projected engineering design wind speed for GEV recurrence period shows that (Figure 9f–h): (i) The V_{d10} for all ports along the Yangtze River inland waterway in flood season of the future scenario shows an increasing trend ($cv > 1$); the rest of the offshore Nanjing–Shanghai section on annual and seasonal scales shows a decreasing trend ($cv < 1$), which is mainly due to the influence of global warming (Figure 9f). (ii)The V_{d50} in the future scenario tends to decrease ($cv < 1$) in the offshore Nanjing–Shanghai section at the annual, dry and normal seasons, while the rest of the ports show an increasing trend; the values of V_{d50} in the future scenario for all ports in the flood season are very close to those in the historical period, indicating that the V_{d50} in the flood season is stationary in the future scenario, which indicates that the effects of global warming on V_{d50} are mainly concentrated in the dry and normal season (Figure 9g). (iii) The spatial distribution of V_d is largely similar over the 50/100 a return period. Under the future scenario, V_{d100} in the offshore Nanjing–Shanghai section tends to decrease under the annual, dry and normal season ($cv < 1$), while the rest of the ports show an increasing trend ($cv > 1$); while V_{d100} in the Chongqing port increases significantly under the normal season ($cv > 1.1$), while the adjacent Yichang port shows a weak decreasing trend ($cv < 1$); in addition, V_{d100} in the midstream (Yueyang–Jiujiang) and coastal areas of the Yangtze River inland waterway during the flood season in Shanghai shows a decreasing trend under the future scenario, while upstream and downstream (noncoastal) areas show an increasing trend ($cv > 1$) (Figure 9h).

4. Discussion

4.1. Main Findings

In this study, we explore the study of differential port engineering design wind speeds for the navigable environment of the YRIW. Due to the large variability in the extreme wind speed characteristics of the Yangtze River inland waterway under the influence of complex climatic factors and topography, the advantages and disadvantages of the Weibull distribution and GEV distribution models are combined with the long time series wind speed data set to analyze the variability about the spatial and temporal distribution of the various models due to the wind climate differentiation. In these port areas, all ports do not follow the Weibull distribution exactly, except for Jiujiang port where the maximum wind speed is closest to the Weibull distribution. The reason is that the Weibull distribution model is a good approximation to the probability density function pdf of surface wind speed under strong wind or unstable stratification conditions, but the Weibull distribution underestimates the wind speed skewness (i.e., underestimates the extremes) under weak wind and stable stratification [28]. In this study, we use the maximum wind speed data set from meteorological stations near each port, most of which include too many low values, resulting in a distribution that does not fully reflect the wind speed distribution characteristics, while the Jiujiang port area is the confluence of Yangtze River and Poyang Lake, which is influenced by the Lushan barrier and the "narrow tube acceleration effect" [29], and has a stable high wind speed that can be applied to the The Weibull distribution model has been applied to the stable high wind speed series. The Weibull method has also been shown to be capable of detecting high wind speed sequences. In this paper, extreme wind speed sample series were extracted from the Weibull distribution using the Tukey method for use in the GEV distribution model, which has been used several times in other studies, although this is the first time it is applied in the study of extreme wind speeds in the Yangtze River inland waterway ports. Based on the results of the goodness-of-fit tests (RMSE and R^2) (Figures 6 and 9), it appears that the method is applicable to this study area. Next, the fitting characteristics of the three distribution types of GEV for each port extreme wind speed at annual and seasonal scales are analysed, and the results also reflect the spatial and temporal characteristics of extreme wind speed at each port, e.g., the type II distribution is more applicable to most of the middle and down streams of the ports with long time series and strong wind–climate mixing complexity, while the type III distribution wind speed distribution is relatively concentrated in some of the upper reaches and Jiujiang ports. The

Gumbel model fails to apply to the annual-scale extreme wind speed of each port, and only applies to the seasonal-scale extreme wind speed during the dry or flood season in Wuhan and Yueyang ports, which is related to the better fitting of the Gumbel distribution when the sample data are normal or exponential type [30]. Based on the effective combination of wind climate and GEV distribution models for each port, it can be deduced at which ports there is a possibility that the engineering design wind speed models and parameters need to be revised due to changes in extreme wind speeds.

A comprehensive analysis of the 10/50/100 a recurrence periods in the study area provides a comprehensive simulation of high precision engineering design wind speed changes under climate change. During the same recurrence period, the pattern of V_d variation with seasons is normal season > dry season > flood season; the high and low value areas vary with seasons, with the high value area expanding from the downstream (dry season) to the midstream (normal season) of the main line, and the low value area expanding from the northern (non-flood) to the southern (flood) part of the Three Gorges Reservoir section; from historical to future periods, the expansion of the high and low value areas from historical to future periods is more obvious. Meanwhile, the intensity and frequency of V_d occurrence are related to topographic features. The "narrow tube acceleration effect" of the topography in the Dongting Lake and Poyang Lake sections has an accelerating effect on the airflow, resulting in a significant increase in wind speed; however, the topography also has a blocking effect on the weather system, resulting in a slowing down of the airflow propagation, as in the Three Gorges reservoir section.

In general, wind speed engineering technology standards are a key aspect of the design of the elements of the Yangtze River navigational environment system and are highly sensitive to extreme weather and climate processes. The wind speed changes in the design of port engineering of navigable environment under climate change are not only related to the safety of Yangtze River shipping infrastructure, but also directly affect the planning and overall development of Yangtze River shipping.

4.2. Limitations of Study Approach

The availability and accuracy of data still need to be improved. For example, there are few data from nearwater stations, which cannot fully reflect the extreme wind speed changes in near-port waters, and it is recommended to strengthen the construction of relevant monitoring stations; obtain at least 30 years of average climate data, and use the encrypted hydrological monitoring stations in the waterway to do accurate wind speed correction, etc.; the spatial and temporal resolution of wind speed products should be further strengthened, by integrating with high-precision and long time series of geographical elements (e.g., land use, impermeable layer). Development of higher resolution wind speed data sets.

The spatial and temporal applicability of wind speed projection for port engineering design needs to be improved. The generalized daily-scale wind speed data cannot obtain accurate 3s and 10s gust data; we can try to carry out small-scale fine modelling through field monitoring work, improve GEV accuracy by using firsthand data, and coupled with other methods, realize the optimization of cumulative distribution function line, improve the prediction accuracy, and then provide higher spatial and temporal resolution of port engineering design wind speed in navigable environment, and provide science for engineering standard design.

The scientific standard of the existing design wind speed for port projects in navigable environments needs to be improved. The extrapolation of the port design wind speed, i.e., the recurrence period wind speed, is the main method of extreme wind speed risk assessment, and the risk assessment process under the influence of different recurrence period wind speeds has certain differences. For example, the research on port engineering design wind speed method is mainly based on the selection of the most suitable fitting model for extreme wind speed in different recurrence periods and the development of extreme wind speed statistical methods, but the research on the optimal wind speed fitting

model for Yangtze River inland waterway navigable environment engineering is not yet seen. In addition, the study of wind speed for port engineering design also involves scientific issues such as variability characteristics and water-land alternation, and there is still a lack of methods that can comprehensively characterize the above scientific issues.

There are still difficulties in collecting, monitoring and verifying high-precision data, and how to carry out adaptation strategies in different types of ports and shipping sections still needs to be studied; extreme wind speed assessment should pay attention to quantification and comprehensiveness, and the assessment of the risk of extreme wind speed changes and the vulnerability risks caused by climate change still needs to be strengthened and should shift from single-factor to multifactor comprehensive assessment, calculating multiple recurrence periods of different extreme weather and climate events in the future from which we should focus on the development of technology to assess the risk of extreme weather and climate hazards at multiple spatial and temporal scales and take into account the economic, social and environmental benefits when formulating climate adaptation measures.

5. Conclusions

In this paper, based on high-resolution wind field data from 1979 to 2100 and the GEV method to derive the engineering design wind speed for the navigable environment with multiscale recurrence periods, the extraction accuracy and distribution of extreme wind speeds with different thresholds are optimized and the method has medium complexity characteristics and extension value.

(1) The maximum wind speed in the YRIW shows a decline—recovery trend in the historical period, with Wuhan, Nanjing and Shanghai stations showing a slight increase except for the dry season.
(2) The maximum wind speed in the study area does not follow the Weibull distribution, and the extracted extreme wind speeds have type I, II and III GEV distributions; the results compared with the Building Load Code show that the updated engineering design wind speeds better reflect the climatic and topographic conditions of the trunk port.
(3) The accuracy of the extreme wind speed projection and the engineering design wind speed will be improved by high-resolution spatial and temporal data and encrypted long-time-series monitoring stations applicability. The wind speed evolution characteristics under different climate change scenarios in the future are predicted, and climate adaptation countermeasures were explored.
(4) The design wind speed of the project was analysed by the high-precision climate model product (CNRM-CM6-1-HR) with an overall increasing trend, and only the design wind speed in the windy areas of Shanghai, Jiujiang and Yueyang showed a weak decrease.

The change in engineering design wind speed of navigation environment under climate change not only concerns the safety of Yangtze River shipping infrastructure but also directly affects the planning and overall development of Yangtze River shipping. By understanding the scientific rules of wind field elements of navigable environment in response to climate change and revealing the extreme wind speed characteristics of the Yangtze River navigable environment in various recurrence periods, this study can provide engineering parameters to support government departments in assessing the design wind speed of Yangtze River inland navigation projects under climate change on the one hand; it can also provide decision-making support for the construction of the Yangtze River Golden Waterway and the planning, design, construction, maintenance and use of Yangtze River inland waterway navigable infrastructure. The results can further serve for the formulation of rules and regulations for the management of mainline navigation, and provide case references and a practical basis for the development strategy of shipping enterprises and the national inland river shipping industry.

Author Contributions: Conceptualization, L.L., J.L. and Y.L.; Formal analysis, J.L. and L.L.; Methodology, Y.L. and L.L.; Software, L.L.; Supervision, L.L. and J.J.; Validation, J.L., L.L. and C.H.; Writing—original draft, J.L. and L.L.; Writing—review and editing, L.L., Y.L. and J.J. All authors have read and agreed to the published version of the manuscript.

Funding: This research was supported by the Science Foundation of the Hubei Province, China (2021CFB295).

Institutional Review Board Statement: Not applicable.

Informed Consent Statement: Not applicable.

Data Availability Statement: Not applicable.

Acknowledgments: Thanks to the anonymous reviewers and the editors for their valuable comments and suggestions.

Conflicts of Interest: The authors declare no conflict of interest.

References

1. Mou, N.X.; Wang, C.Y.; Yang, T.F.; Zhang, L.X. Evaluation of development potential of ports in the Yangtze River delta using FAHP-entropy model. *Sustainability* **2020**, *12*, 493. [CrossRef]
2. Lung, T.; Lavalle, C.; Hiederer, R.; Dosio, A.; Bouwer, L.M. A multi-hazard regional level impact assessment for Europe combining indicators of climatic and non-climatic change. *Glob. Environ. Chang.* **2013**, *23*, 522–536. [CrossRef]
3. Sardain, A.; Sardain, E.; Leung, B. Global forecasts of shipping traffic and biological invasions to 2050. *Nat. Sustain.* **2019**, *2*, 274–282. [CrossRef]
4. Baroud, H.; Barker, K.; Ramirez-Marquez, J.E. Importance measures for inland waterway network resilience. *Transp. Res. Part E Logist. Transp. Rev.* **2014**, *62*, 55–67. [CrossRef]
5. Verschuur, J.; Koks, E.E.; Hall, J.W. Port disruptions due to natural disasters: Insights into port and logistics resilience. *Transp. Res. Part D-Transp. Environ.* **2020**, *85*, 102393. [CrossRef]
6. Liu, L.J.; Wen, Y.Q.; Liang, Y.J.; Zhang, F.; Yang, T.T. Extreme weather impacts on inland waterways transport of Yangtze River. *Atmosphere* **2019**, *10*, 133. [CrossRef]
7. Christodoulou, A.; Christidis, P.; Bisselink, B. Forecasting the impacts of climate change on inland waterways. *Transp. Res. Part D-Transp. Environ.* **2020**, *82*, 102159. [CrossRef]
8. Gray, S.R.J.; Gagnon, A.S.; Gray, S.A.; O'Dwyer, B.; O'Mahony, C.; Muir, D.; Devoy, R.J.N.; Falaleeva, M.; Gault, J. Are coastal managers detecting the problem? Assessing stakeholder perception of climate vulnerability using Fuzzy Cognitive Mapping. *Ocean Coast. Manag.* **2014**, *94*, 74–89. [CrossRef]
9. Natarajan, N.; Vasudevan, M.; Rehman, S. Evaluation of suitability of wind speed probability distribution models: A case study from Tamil Nadu, India. *Environ. Sci. Pollut. Res.* **2021**, *14*, 1–14. [CrossRef]
10. Xiang, C.; Chen, A.R.; Li, Q.H.; Ma, R.J. Research on the probability model of basic wind speed estimation in China. *Wind Struct.* **2021**, *32*, 587–596. [CrossRef]
11. Yahaya, A.S.; Nor, N.; Jali, N.R.M.; Ramli, N.; Ahmad, F.; Ul-Saufie, A.Z. Determination of the Probability Plotting Position for Type I Extreme Value Distribution. *J. Appl. Sci.* **2012**, *12*, 1501–1506. [CrossRef]
12. Sarkar, A.; Deep, S.; Datta, D.; Vijaywargiya, A.; Roy, R.; Phanikanth, V.S. Weibull and Generalized Extreme Value Distributions for Wind Speed Data Analysis of Some Locations in India. *Ksce J. Civ. Eng.* **2019**, *23*, 3476–3492. [CrossRef]
13. Perrin, O.; Rootzén, H.; Taesler, R. A discussion of statistical methods used to estimate extreme wind speeds. *Theor. Appl. Climatol.* **2006**, *85*, 203–215. [CrossRef]
14. Gumbel, E. Statistics of extremes. In *Statistics of Extremes*; Columbia University Press: New York, NY, USA, 1958.
15. Simiu, E.; Yeo, D. *Wind Effects on Structures: Modern Structural Design for Wind*; John Wiley & Sons: New York, NY, USA, 2019.
16. Roslan, R.; Chin, S.N.; Gabda, D. Parameter Estimations of the Generalized Extreme Value Distributions for Small Sample Size. *Math. Stat.* **2020**, *8*, 47–51. [CrossRef]
17. Kumar, D.; Mishra, V.; Ganguly, A.R. Evaluating wind extremes in CMIP5 climate models. *Clim. Dyn.* **2015**, *45*, 441–453. [CrossRef]
18. Van den Hurk, B.; Tank, A.K.; Lenderink, G.; Ulden, A.V.; Oldenborgh, G.J.V.; Katsman, C.; Brink, H.V.D.; Keller, F.; Bessembinder, J.; Burgers, G.; et al. New climate change scenarios for the Netherlands. *Water Sci. Technol.* **2007**, *56*, 27–33. [CrossRef]
19. De Winter, R.C.; Sterl, A.; Ruessink, B.G. Wind extremes in the North Sea Basin under climate change: An ensemble study of 12 CMIP5 GCMs. *J. Geophys. Res.-Atmos.* **2013**, *118*, 1601–1612. [CrossRef]
20. Roberts, M.J.; Camp, J.; Seddon, J.; Vidale, P.L.; Hodges, K.; Vanniere, B.; Mecking, J.; Haarsma, R.; Bellucci, A.; Scoccimarro, E.; et al. Impact of model resolution on tropical cyclone simulation using the HighResMIP-PRIMAVERA multimodel ensemble. *J. Clim.* **2020**, *33*, 2557–2583. [CrossRef]
21. Liu, L.J.; Zhang, F. Spatiotemporal Dynamics of Maximum Wind Speed Using the Wind Multiplier Downscaling Method in the Yangtze River Inland Waterway from 1980 to 2017. *Atmosphere* **2021**, *12*, 1216. [CrossRef]

22. Simmons, A.J.; Willett, K.M.; Jones, P.D.; Thorne, P.W.; Dee, D.P. Low-frequency variations in surface atmospheric humidity, temperature, and precipitation: Inferences from reanalyses and monthly gridded observational data sets. *J. Geophys. Res.-Atmos.* **2010**, *115*, D1. [CrossRef]
23. Liu, L.J.; Liang, Y.J. Wind power forecast optimization by integration of CFD and Kalman filtering. *Energy Sources Part A-Recover. Util. Environ. Eff.* **2021**, *43*, 1880–1896. [CrossRef]
24. Fisher, R.A.; Tippett, L.H.C. Limiting forms of the frequency distribution of the largest or smallest member of a sample. In *Mathematical* Proceedings of the Cambridge Philosophical Society; Cambridge University Press: Cambridge, UK, 1928; pp. 180–190.
25. Tukey, J.W. *Exploratory Data Analysis*; Addison-Wesley: Reading, MA, USA, 1977; Volume 2.
26. Wilks, D.S. *Statistical Methods in the Atmospheric Sciences*; Academic Press: Cambridge, UK, 2011; Volume 100.
27. Hosking, J.R.M.; Wallis, J.R.; Wood, E.F. Estimation of the generalized extreme-value distribution by the method of probability-weighted moments. *Technometrics* **1985**, *27*, 251–261. [CrossRef]
28. Shi, H.Y.; Dong, Z.B.; Xiao, N.; Huang, Q.N. Wind Speed Distributions Used in Wind Energy Assessment: A review. *Front. Energy Res.* **2021**, *9*, 790. [CrossRef]
29. Hu, C.L.; Zhang, Y.F.; Jiang, Z.X.; Wang, M.; Han, C. Development of large-scale sand bodies in a fault-bounded lake basin: Pleistocene-Holocene Poyang Lake, Southern China. *J. Paleolimnol.* **2021**, *65*, 407–428. [CrossRef]
30. Kang, D.; Ko, K.; Huh, J. Determination of extreme wind values using the Gumbel distribution. *Energy* **2015**, *86*, 51–58. [CrossRef]